Delay modeling of a multihop broadcast protocol for vehicular networks

Te Yan

June 5, 2025

Abstract

With the increasing adoption of intelligent transportation systems, vehicle-to-vehicle (V2V) communication in dynamic highway environments has emerged as a key research area. Due to the highly mobile and rapidly changing topology of vehicular ad hoc networks (VANETs), understanding their performance under varying conditions is critical. In this study, we model and analyze the average one-hop delay and reliability—two essential metrics for evaluating the effectiveness of safety packet dissemination in V2V communication scenarios.

Index Terms—VANETs, Broadcast, One-hop delay, CSMA/CA, Reliability

Contents

Chapter 1

Introduction

1.1 Related Works

1. There are several protocols align our work. At first, we present several protocols that share similar functionalities and are designed for message dissemination among vehicles. They could be devided into three categories. The first category is time-based multi-hop protocols. In the protocol proposed by Briesemeister [1], the waiting time of each forwarding candidate is inversely proportional to its distance from the previous forwarding node. To overcome the issues of hidden nodes and efficient forwarder selection in vehicular environments, the Urban Multi-hop Broadcast (UMB) [2] protocol was introduced. A protocol called DEEP [3] assumes that each vehicle is aware of its own location and the region it belongs to. When a vehicle receives a new emergency message, it computes and waits for a deferral time, which is determined by the distance from the source vehicle to the current region and the size of the region. DEEP has been reported to effectively address the broadcast storm problem. Another multi-hop broadcast protocol designed to address the same issue is the Robust and Fast Forwarding (ROFF) [4] protocol, which avoids transmission collisions among potential forwarding candidates (PFCs) by calculating appropriate waiting times. Second network coding is designed to enable each intermediate node to mix different received packets before forwarding them. References [5] and [6] are representative works in this area. Third, the approach we adopt belongs to the Probability-Based Multi-Hop broadcast category. All the protocols mentioned here assign the forwarding probability of each node based on its distance from the source node. The forwarding strategies in [8] and [9] are derived from the same probability formula, as:

   $$p = \left(\frac{d}{R}\right)^k \tag{1.1}$$

   Reference [8] considers the specific case where $k = 1$, whereas [9] extends the formula by allowing a variable coefficient k, thereby enabling more flexible control over the forwarding probability. In addition, two other protocols incorporate vehicle density into the forwarding probability. Specifically, [10] introduces the following formula as

   $$p = e^{-\rho_s \cdot \left(\frac{R-d}{c}\right)} \tag{1.2}$$

where ρ represents the estimated local vehicle density, c is the coefficient. [11] introduces an enhanced density-aware forwarding probability model as

$$p = e^{-\rho_s \cdot \left[\frac{R-d}{c}\right] \cdot \left(\frac{R}{R_i}\right)} \tag{1.3}$$

where R_i is the transmission range of the i-th receiving vehicle. The protocols in [10] and [11] are particularly suitable for VANET highway scenarios because they take vehicle density into account, which is a relatively important factor in highway environments.

2. The performance of CSMA/CA has been widely studied, and in our work, we refer to the following findings to support our analysis. First, we refer to the Bianchi model [14], which is the first to formally introduce a Markov chain-based analytical model for the CSMA/CA mechanism, providing a foundational framework for evaluating its performance. However, the aforementioned work concentrates on saturated network conditions. In contrast, our study addresses bursty traffic patterns characteristic of safety packet transmissions, necessitating an analysis of the protocol's behavior under unsaturated conditions. For unsaturated scenarios, we utilize the model presented by Malone [15], which describes the behavior of CSMA/CA networks in the absence of packets awaiting transmission. From the aforementioned works, we have gained an understanding of the fundamental principles of Markov chains and how they can be applied to model various behaviors (e.g. transmitting, awaiting packets, etc.) within the CSMA/CA mechanism. Second, for the estimation of the average one-hop delay under steady-state conditions, we refer to the work by Ma [13], where the mean value is used to represent the delay. This work analyzes the characteristics of network nodes and the CSMA/CA mechanism, and summarizes the network performance under steady-state conditions through extensive simulation experiments.

3. Reliability is likewise an essential performance metric in VANETs, particularly in the context of safety (emergency) packet dissemination. In this context, the most critical aspect lies in how reliability is defined as a performance metric. In this context, we define reliability as the probability that a vehicle successfully receives the message. We aim to measure the average broadcast reception probability of vehicles at various locations within the dissemination range of the broadcast message. To evaluate the reliability we have measured, we adopt the definition of reliability proposed in [17], specifically the concept of coverage in our work, to verify whether our proposed and measured reliability is reasonable.

1.2 Contributions

In our work, we propose a novel average one-hop delay model for multi-hop broadcast protocols under the scenario described in FPBCSN, along with an analysis of the reliability based on vehicle density within this model.

1. We provide a more accurate modeling of the average one-hop delay for the FPBCSN protocol. Previous models were designed for saturated networks; however, the FPBCSN protocol operates under an unsaturated network scenario. Therefore, our model can more precisely characterize the dissemination behavior of emergency messages on highways.

2. It is also necessary to model the reliability—defined as the probability of successful message reception by a vehicle—in order to ensure stable network performance.

3. Building upon the reliability model, we further model the network coverage as a function of varying vehicle density. This serves as an indirect validation of the reliability model and provides insight into the performance variations under different vehicle densities.

Chapter 2

The Scenario, Network Modeling and Problem Statement

2.1 Network Modeling

The network model employed in this study is introduced in this section. In our scenario, we make the following assumptions:

- A fixed transmission range is assigned to each vehicle, and it is denoted by R. The one-hop distance is defined as R, oriented in the direction opposite to the movement of the vehicles.
- The vehicles are assumed to be uniformly distributed along a single-lane highway, where N represents the number of vehicles located within the one-hop transmission range.
- Each vehicle is equipped with a distance-measuring radar, which allows it to identify the number of neighboring vehicles within one-hop range and accurately estimate their distances.

As illustrated in Fig. 2.1, we consider a scenario of a straight highway. Within a one-hop transmission range, all N vehicles are considered potential forwarding candidates. The FPBCSN protocol is designed to select actual forwarding nodes from among these

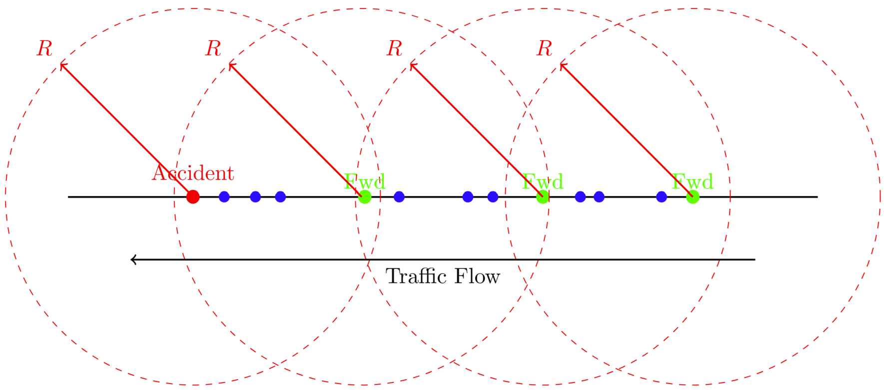

Figure 2.1: Demonstration of a message forwarding scenario

candidates. The source node, denoted as Accident, represents the occurrence of a traffic accident. Vehicles located within one hop of the source need to be notified via an emergency message broadcast. Among these vehicles, the selected forwarding nodes are responsible for rebroadcasting the received emergency message to vehicles further behind, thereby achieving the goal of alerting nearby traffic. The ideal scenario is to have the farthest one or few vehicles within the one-hop range serve as the forwarding nodes. This ensures efficient long-distance information dissemination while minimizing channel contention and transmission delays, which could result from having too many broadcasting nodes in a small area. Fig. 2.1 illustrates this ideal case.

2.2 Problem Statement

In this work, our objective is to model the average one-hop delay of the FPBCSN protocol and to compute its reliability.

The one-hop delay in CSMA/CA mechanism is not a precise or fixed value, which decided by each node exponential binary backoff procedure. Our objective is to calculate the expected number of forwarding nodes given that each potential forwarder, selected by the source node, is assigned a forwarding probability p_i. Based on the average number of forwarders in a single hop, we estimate the total number of forwarding nodes across the entire network. This allows us to derive the probability of channel contention in the network and, subsequently, to estimate the average duration of the backoff process encountered during the dissemination of an emergency packet. Ultimately, this leads to the computation of the average one-hop delay.

Then our study focuses on analyzing the reliability of the network. Reliability refers to the probability that each vehicle successfully receives the message transmitted by the source node. To this end, we incorporate a small-scale fading model (Nakagami) on top of the existing large-scale path loss model to capture the randomness in message reception at the nodes. This enables a detailed examination of each vehicle's likelihood of successfully receiving the broadcast information.

Although the reception rate has been addressed, evaluating network performance under different vehicle densities remains essential through further modeling efforts. Therefore, it is necessary to investigate the broadcast coverage under varying vehicle densities to characterize the overall network performance when small-scale fading effects are considered.

Chapter 3

The Proposed Multi-Hop Broadcast Protocol

3.1 Protocol Description

To optimize emergency message dissemination in vehicular networks by reducing redundant broadcasts, average one-hop delay and maintain coverage efficiency, we use the FPBCSN [16], a distance-aware probabilistic forwarder selection protocol.

$$p_i = \lambda \cdot \left(\frac{1}{i}\right)^k, for\ i \in \mathbb{Z} \tag{3.1}$$

where i is the vehicle sequential number, λ is the probability coefficient, k is the power exponent to adjust the forwarding probabilities among the nodes contending for the broadcast channel. In our proposal, the optimal broadcast strategy involves selecting the vehicle with index $i = 1$ in each hop for message forwarding, thereby maximizing the propagation range while minimizing channel contention. As Fig. 3.1 and 3.2, we can compare the forwarding probability among the protocols we suggested. We can observe that the advantage of the protocol we used lies in the fact that the specific distance does not affect our forwarding probability

3.2 Average One-Hop Delay

In our work, we decreased the number of forwarders, but we need to evaluate it for modeling the channel contention based on it. We denote the expected number of forwarders as N_f, the expression of N_f as:

$$N_f = \lambda \sum_{i=1}^{n} \frac{1}{i} \tag{3.2}$$

We observe how the expected number of forwarders changes with changing vehicle density n, ranging from 5 to 50. We use different coefficients, as Fig. 3.3, the coefficients are $\lambda = 0.9$, $k = 1$.

As Fig. 3.4, with λ held constant and $k = 3$, the value of N_f decreases and its rate of change smaller than $k = 1$. This is because, when $k = 3$, the forwarding probability of all nodes, except for the farthest node, decreases.

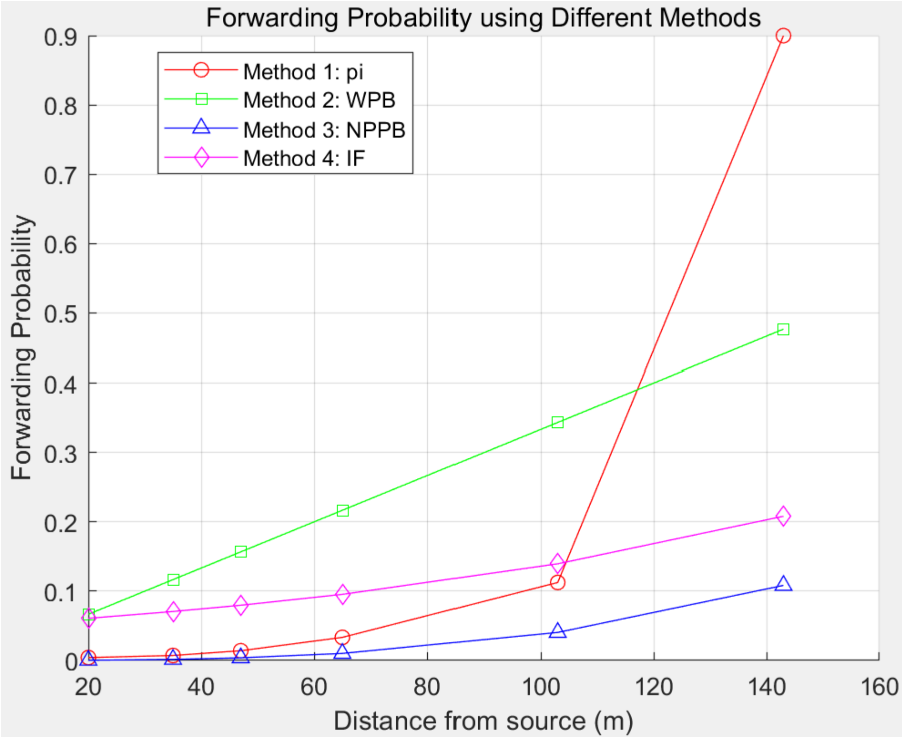

Figure 3.1: Protocols Forwarding Probability Comparison

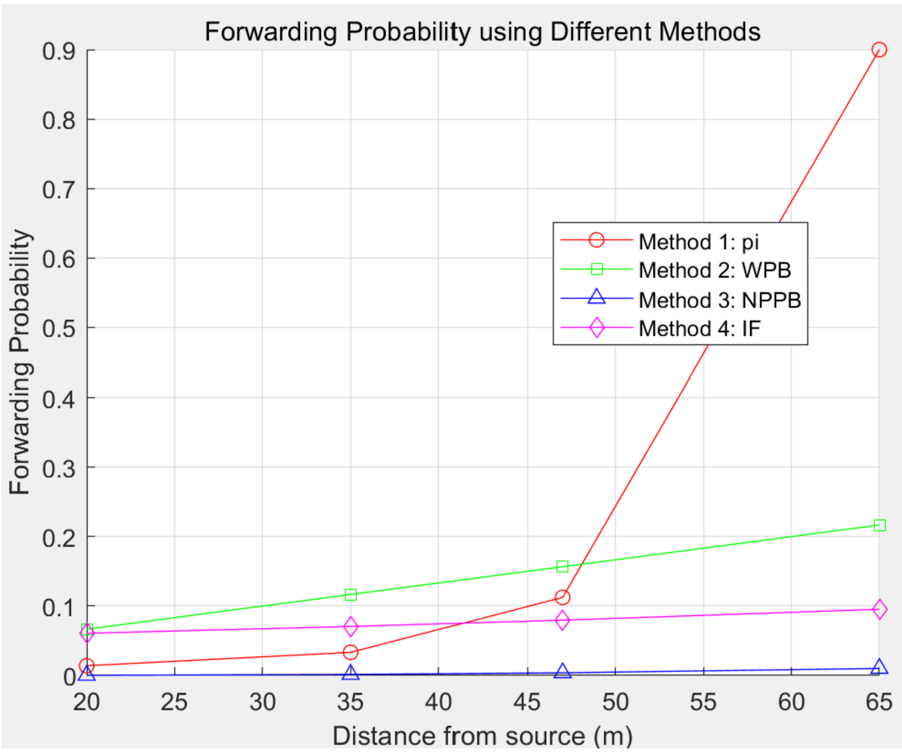

Figure 3.2: Protocols Forwarding Probability Comparison (loss of the farthest node)

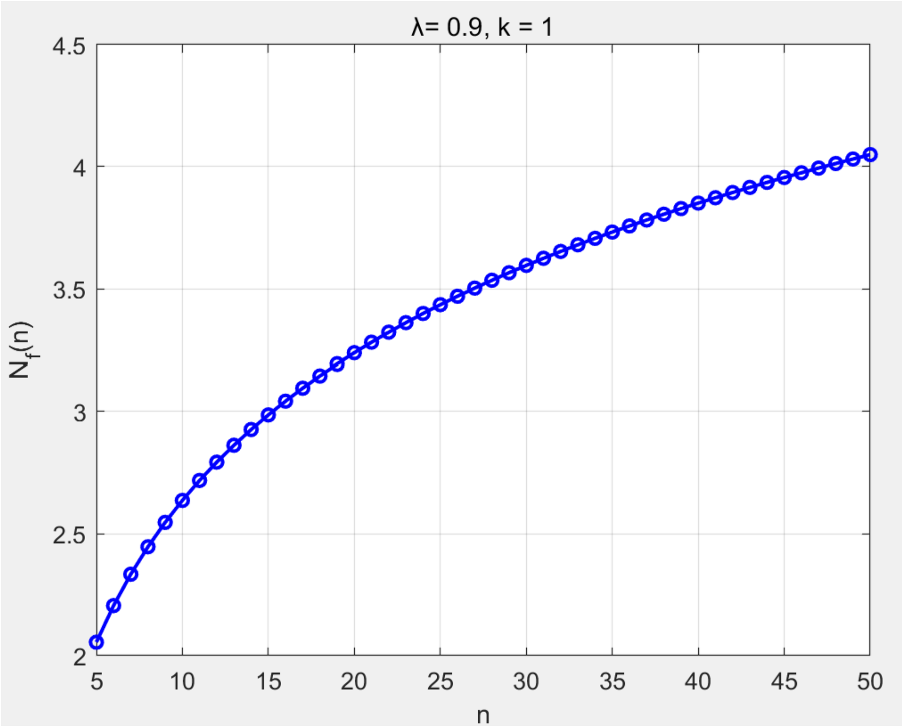

Figure 3.3: $\lambda = 0.9,\ k = 1.0$

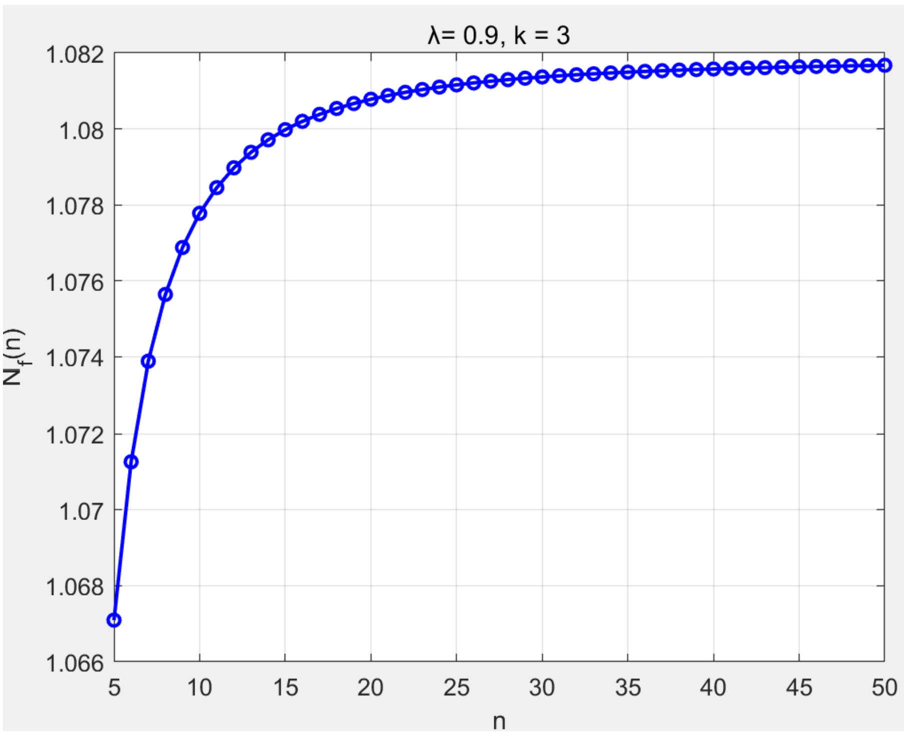

Figure 3.4: $\lambda = 0.9,\ k = 3.0$

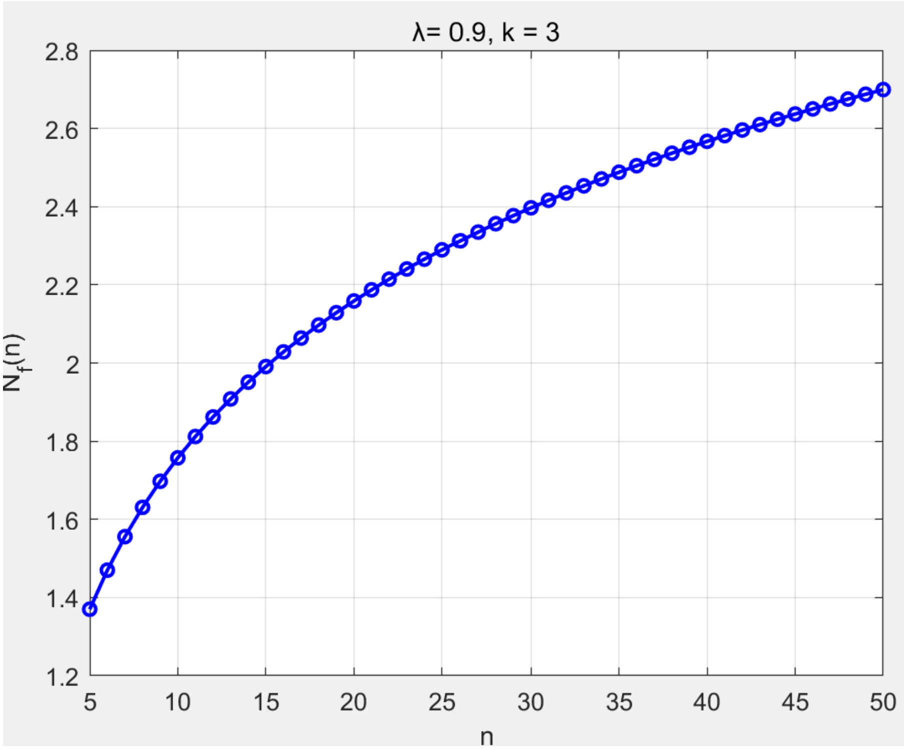

Figure 3.5: $\lambda = 0.6$, $k = 1.0$

When $\lambda = 0.6$, and $k = 1$ and 3, we obtain similar results. In this case, the value of N_f is generally smaller than $\lambda = 0.9$ as the forwarding probability of all vehicles has decreased. As Fig. 3.5 and 3.6.

3.2.1 The Delay Without MAC Contention

In one of our scenarios, the channel contention on MAC layer would not be considered. This scenario refers to the case where we compute the average one-hop delay based only on the delay of the first successfully received packet, other packets with the same packet ID as the first received packet are discarded. The Eq. 3.3 is the average time that the channel is sensed busy and collision according to [16].

$$T = \frac{L_H + E[P] + 12}{R_d} \times 8 + \text{DIFS} + \delta \tag{3.3}$$

In Eq. 3.3, the L_H is Physical and MAC layer header, The $E[P]$ is average packet size,the value 12 accounts for the additional information appended to each packet, namely a packet ID and a timestamp. The packet ID is stored as an integer (4 bytes) and the timestamp as a double (8 bytes) in C++, resulting in a total of 12 bytes.

In our method, we append the forwarder's node ID, converted into a byte stream, to the end of each packet. Since an integer occupies 4 bytes, we add $N_f * 4$ to the numerator of the expression. As

$$T = \frac{L_H + E[P] + N_f \times 4 + 12}{R_d} \times 8 + \text{DIFS} + \delta \tag{3.4}$$

However, the Eq. 3.4 still fails to accurately match the simulation results. As shown in Fig. 4.1 to Fig. 4.4, it can be observed that there is always a certain gap between

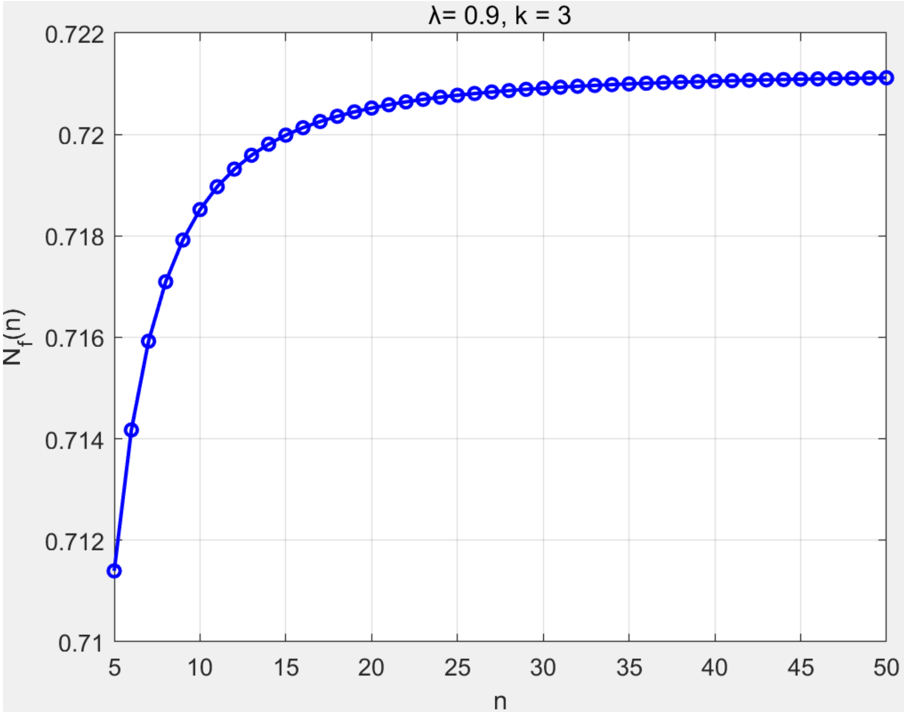

Figure 3.6: $\lambda = 0.6$, $k = 3.0$

the simulation results and the theoretical results when different packet sizes are used. However, through observation and calculation, it is found that the difference between the simulation and theoretical results remains almost constant across different packet sizes. In the previous work [16], we did not account for the headers of network layers other than the physical and MAC layers. Here, we denote $E[S]$ as the size of the headers from other layers, and through calculation, we find that $E[S]$ is approximately 58.5 bytes. Therefore, the complete expression for T should be

$$E[D] = T = \frac{L_H + E[P] + E[S] + N_f \times 4 + 12}{R_d} \times 8 + \text{DIFS} + \delta \tag{3.5}$$

In this case, T is equivalent to the average one-hop delay, $E[D]$, as MAC channel contention has not been taken into account. The difference between the simulation and theoretical values is caused by the binary exponential backoff mechanism. In this mechanism, a random backoff state is selected, meaning the number of waiting slots (σ) is a random value. However, in our scenario, each node only receives the first broadcast packet with a given packet ID, and ignores any duplicates. This implies that the node which selects the smallest number of σ will transmit first and be received by others. Therefore, the simulation reflects the minimum backoff time among contending nodes, which is not fully captured by the theoretical model, leading to a deviation between the two results.

In fact, our estimated value of $E[S]$ is slightly larger. This adjustment is intentional to make the theoretical results match the minimum observed values in the simulation. Since our model does not account for the number of time slots σ that a packet may undergo during the transmission process due to backoff, the increased $E[S]$ compensates for this omission and improves the alignment between theoretical and simulation results.

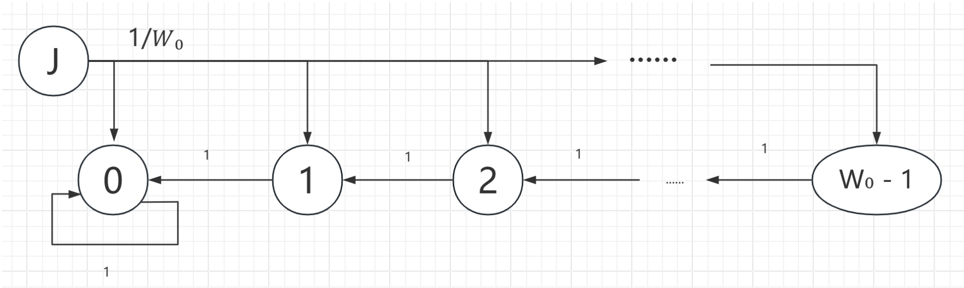

Figure 3.7: Markov Chain Model

3.2.2 The Delay With MAC Contention

If we consider the MAC contention influence, although packets with the same packet ID as previously received ones are discarded, we still record the delay of every received packet. This ensures that the impact of channel contention on delay is fully reflected when calculating the average one-hop delay.

For the MAC layer delay, its mechanism exhibits Markov chain characteristics; therefore, we need to use a Markov model, as shown in Fig. 3.7, to describe it.

$$P[K|J] = \frac{1}{W_0} \tag{3.6}$$

$$P[K-1|K] = 1 \tag{3.7}$$

$$P[0|0] = 1 \tag{3.8}$$

From Fig. 3.7, we derive the transition relationships between each state, as shown in Eqs. 3.6 to 3.8.

$$\frac{b(0)}{b(J)} = \frac{1}{W_0} \Rightarrow b(J) = W_0 \cdot b(0) \tag{3.9}$$

$$\frac{b(W_0-1)}{b(J)} = \frac{1}{W_0} \tag{3.10}$$

From Eqs. 3.9 and 3.10, we derive the relationship between $b(J)$ and $b(0)$, establishing the connection between $b(J)$ and other states.

$$b(W_0-1) = \frac{b(J)}{W_0} = b(0) \tag{3.11}$$

$$b(W_0-2) = \frac{b(J)}{W_0} + b(W_0-1) \cdot 1 = 2b(0) \tag{3.12}$$

$$b(W_0-3) = \frac{b(J)}{W_0} + b(W_0-2) \cdot 1 = 2b(0) \tag{3.13}$$

......

$$b[W_0-(W_0-1)] = b(1) = \frac{b(J)}{W_0} + b(2) \cdot 1 = (W_0-1)b(0) \tag{3.14}$$

$$b(0) \tag{3.15}$$

From Eqs. 3.11 to 3.15, the relationships between $b(1)$ to $b(W_0 - 1)$ and $b(0)$ are established. Based on the properties of the Markov chain, we obtain Eq. 3.16.

$$b(J) + \sum_{k=0}^{W_0-1} b(k) = 1 \tag{3.16}$$

By combining the previous equations, we obtain Eq. 3.17.

$$b(0) \cdot \left[\frac{W_0 \cdot (W_0 - 1)}{2} + 1 + W_0 \right] = 1 \tag{3.17}$$

Since $b(0)$ is the final state in the entire Markov chain, according to [14] and [15], we know that τ, which is the stationary distribution's probability that the station transmits in a slot, is equal to $b(0)$. So we can get the expression of τ as Eq. 3.18.

$$\tau = b(0) = \frac{1}{\left[\frac{W_0(W_0-1)}{2}\right] + 1 + W_0} \tag{3.18}$$

We denote p_b as the probability that the channel is busy. The channel becomes busy due to multiple nodes attempting to transmit simultaneously, during which the CSMA/CA mechanism operates to avoid collisions. As our scenario requires three-hop propagation, we collect the average one-hop delay for all packets across the three hops. Accordingly, we need to estimate the number of forwarding nodes, namely those participating in channel contention.

$$p_b = 1 - (1 - \tau)^{(N_f + N_f^2 + N_f^2)/3} \tag{3.19}$$

In [13], n is used to represent the number of nodes participating in contention. In our scenario, if only the first hop is considered without accounting for farther nodes, it would be sufficient to use N_f directly. However, since we need to consider that all forwarding nodes within three hops may participate in forwarding, we use $(N_f + N_f^2 + N_f^2)/3$ to represent the average number of forwarding nodes, i.e., the number of nodes participating in channel contention. N_f^2 represents the number of forwarding nodes selected by the forwarding nodes determined at the first hop for the next hop. However, at the third hop, using N_f^3 would exceed the range of nodes arranged for the third hop. Thus, we also adopt N_f to represent the number of forwarding nodes at the third hop, achieving a more accurate model. This is further supported by our simulation observations, where the number of forwarding nodes at the third hop is found to be approximately N_f^2. The expression for p_i is shown in Eq. 3.19.

$$E[D] = T + \frac{W_0}{2} \times [(1 - p_b)\sigma + p_b T] \tag{3.20}$$

In [13], an average one-hop delay is obtained through an estimation based on expected values. However, in our work, p_b is a very small value, while the delay T when a node transmits a packet is always present. Therefore, following the approach in [13] for $E[D]$, we compute the expected value by considering the state transitions with uncertain delays σ and T, from $b(1)$ to $b(W_0 - 1)$. The expected value of states changing derivation is

$$\frac{(1+W_0-1)}{2}\cdot\frac{(W_0-1)}{(W_0-1)}=\frac{W_0}{2}$$

Based on this, we derive the new average one-hop delay estimation formula, given in Eq. 3.20.

3.2.3 Reliability

The reliability means the probability of a message being received by a vehicle. In our previous work, only a large-scale fading model was used, so whether a downstream node could receive the broadcast message after each transmission was a deterministic event, given a fixed distance. This assumption leads to a significant deviation from realistic wireless communication environments. Accordingly, we augment the large-scale fading model by sequentially integrating a small-scale fading component, in order to better capture real-world signal fluctuations that may prevent some vehicles from successfully receiving broadcast messages.

Currently, we employ the Log-Distance Path Loss Model as the large-scale fading model, and the Nakagami model as the small-scale fading component. The equation of the Log-Distance Path Loss Model as

$$PL(d)=PL(d_0)+10\cdot n\cdot\log\left(\frac{d}{d_0}\right)+X_\sigma \tag{3.21}$$

In our scenario, we ignore the component X_σ. The small-scale fading model is implemented by multiplying the linear-scale received power from the large-scale fading model with the square of a Nakagami-distributed random coefficient, in order to simulate the stochastic variations of the signal strength. The multiplication coefficient is denoted as r, it observes as

$$f(r)=\frac{2m^m}{\Gamma(m)\Omega^m}r^{2m-1}\exp\left(-\frac{mr^2}{\Omega}\right),\quad r\geq 0 \tag{3.22}$$

which means $r\sim$ Nakagami(m,Ω). The r^2 is the coefficient to affect the receive power, r^2 means power fluctuation.

The Fig. 3.8 presents the Loss Path Model with the Nakagami model.

3.3 Coverage

Based on the measured reliability, the network coverage can be estimated. In our scenario, the Nakagami fading model is employed to simulate radio signal fluctuations, which are categorized into three distinct fading regions. The three regions are defined based on distance from the source as 0–100 m, 100–200 m, and 200–300 m. Within one hop (300 meters), there are n vehicles randomly distributed over the range of 0 to 300 meters. Each vehicle is assigned a transmission probability p_i, which is determined based on its relative distance to the source node. Consequently, each vehicle within the one-hop range also has an associated probability of being located in one of the three subregions: 0–100 m, 100–200 m, and 200–300 m. We denote this location-based probability as p_{loci}. We provide the following explanation for determining the region in which each vehicle is likely to be located. We assume that X_1, X_2,..., X_n Uniform (0, 300), representing the

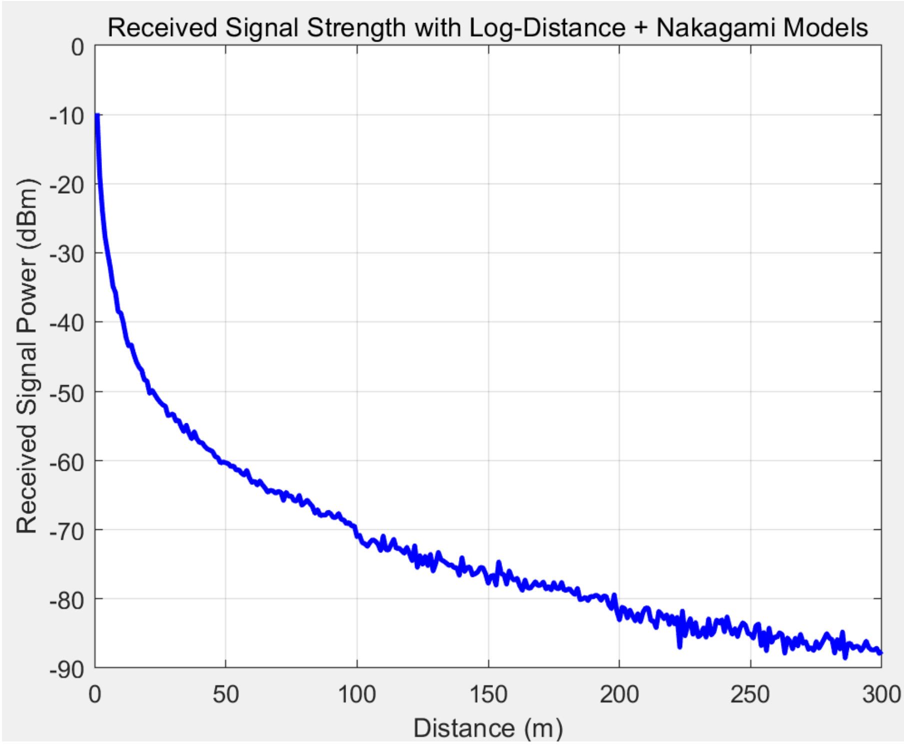

Figure 3.8: Logdistance and Nakagami Receive Power

positions of the n vehicles uniformly distributed within the one-hop range. To characterize the distribution of vehicles within the specified range, we employ the Beta distribution, which allows flexible modeling of spatial variability and ordering. The Beta distribution we present that as

$$X_{(k)} \sim \text{Beta}(k, n-k+1) \cdot L \tag{3.23}$$

Here, n denotes the number of nodes within the one-hop range, and k represents the index of the k-th order statistic (k corresponds to the ordering of vehicles from the nearest to the farthest relative to the source node). Let $X_{(k)}$ denote the k-th order statistic of n independent and identically distributed vehicle positions. Its probability density function is given as

$$f_{X_{(k)}}(x) = \frac{n!}{(k-1)!(n-k)!} \left(\frac{x}{L}\right)^{k-1} \left(1 - \frac{x}{L}\right)^{n-k} \cdot \frac{1}{L} \tag{3.24}$$

We use the probability density function $f_{X_{(k)}}(x)$ to calculate the probability that each vehicle is located within a specific subregion of the road, corresponding to different values of the Nakagami-m parameter.

Therefore, to compute the average reception probability for each vehicle, we combine the probability p_{loci} that the vehicle is located in each subregion with the corresponding average reception probability p_{rc} of that region (associated with a specific Nakagami-m value). The resulting average reception probability is given as

$$P_{\text{Ravg},i} = \sum_{c=1}^{3} p_{\text{loc}}(i, c) \cdot p_{\text{rc}}(c) \tag{3.25}$$

Here, the index i in $p_{loc}(i, c)$ corresponds to the vehicle identifier, which is the same as in p_i. The index c denotes the subregion within the one-hop range characterized by different Nakagami-m values. We define these subregions as $c = 1, 2, 3$, corresponding to the distance intervals of 0–100 m, 100–200 m, and 200–300 m, respectively.

Now that we have obtained the average reception probability $P_{Ravg,i}$ and the transmission probability p_i for each vehicle, we aim to determine the probability that a message is successfully forwarded in a given hop. Specifically, successful forwarding occurs if at least one vehicle both receives and transmits the message. Given that the probability of transmission failure due to contention (with $CW_0 = 15$) is relatively low, as suggested in [16], we neglect such collisions in our analysis. Therefore, the probability that a single vehicle successfully forwards a message is given by $P_{Ravg,i} \cdot p_i$. Consequently, the probability that this vehicle does not forward the message is $1 - P_{Ravg,i} \cdot p_i$. Assuming independence among vehicles, the probability that none of the n vehicles in the hop forwards the message is

$$P_{\text{None}} = \prod_{i=1}^{n} (1 - P_{\text{Ravg},i} \cdot p_i) \tag{3.26}$$

The probability that at least one vehicle transmits is obtained by subtracting the probability that none of the vehicles transmit from 1. Therefore, based on Eq. 3.26, we can derive the probability that at least one vehicle successfully forwards the message within a single hop as

$$P_{\text{avgsnd}} = 1 - P_{\text{None}} \tag{3.27}$$

This expression represents the probability that a message is successfully forwarded from one hop to the next. The only exception is the transmission from the source node to the first-hop vehicles, where the transmission probability is assumed to be 1, since all first-hop vehicles are within the communication range of the source. This theoretical result will be validated through simulation experiments, where the probability of successful message forwarding is observed to increase as the number of nodes within one hop increases. It can be observed that the product $P_{Ravg,i} \cdot p_i$ is generally small for individual vehicles. Consequently, the term $1 - P_{Ravg,i} \cdot p_i$ tends to be relatively large. However, when multiple such terms—each less than one—are multiplied together, the overall product P_{None} decreases as the number of vehicles n within one hop increases. As a result, the probability that at least one vehicle successfully forwards the message, defined as $P_{avgsnd} = 1 - P_{None}$, increases with larger n.

To evaluate the average coverage over three hops, we consider the proportion of nodes that successfully receive the message across all hops, assuming it propagates at least three hops. According to Eq. 3.27, the probability that a message is forwarded from one hop to the next is denoted as P_{avgsnd}. Since the source node successfully transmits to the first hop with probability 1, the expected coverage over three hops can be expressed as

$$P_{\text{covg}}(3 \text{ hops}) = \frac{1}{3} \sum_{d=1}^{3} \lambda^{d-1} \tag{3.28}$$

This formula can be generalized to an arbitrary number of hops, resulting in the following expression for the coverage over H_P hops:

$$P_{\text{covg}} = \frac{1}{H_P} \sum_{d=1}^{H_P} \lambda^{d-1} \tag{3.29}$$

Here, H_P denotes the maximum number of hops, which is set to three in our scenario, H_P is just a generalized version.

Chapter 4

Simulations and Results

4.1 Simulation Configuration

The simulations are conducted to verify the proposed average one-hop delay model in the FPBCSN broadcast protocol for vehicular network. The simulator is NS-3 version 3.37. Our simulation follows the WAVE with IEEE 802.11p standard. All the parameters of MAC layer we used are default by WAVE module in NS-3.37 and summarized in Table I. In our scenario, we used the one-way straight highway model with 1 lane, the lane width is $10m$, length is $900m$. There are 5 50 vehicles uniformly distributed within the transmission range of the source node. The speed of these vehicles are $30m/s$. The source and forwarders transmit an emergency packet every 0.1 second, with a total of three transmissions. The total simulation time is $20s$. We set the transmission range to a fixed value of $300m$, as, according to Chinese highway regulations, emergency signs should be placed $150m$ behind the accident site. Therefore, we set the transmission range to twice the Chinese standard, resulting in $300m$.

4.2 Simulation Challenges

There are several challenges encountered in our simulation.

- We need to determine the header length at each network layer, from the physical layer to the application layer. The header lengths of the physical and MAC layers are obtained from [16], while those of the other layers are derived from the simulation results. Since the transmission rate is expressed in bits per second, it is necessary to specify the number of bits for each layer's header.

- We need to use a class to configure the application layer of each vehicle, setting up the functions for receiving and sending at the application layer, with particular emphasis on probability calculation, information acquisition, and periodic Sending.

- A key challenge in information dissemination is the integration of necessary information into packets, either by attaching tags or by directly appending data to the packet payload.

- The calculation of the average one-hop delay is also a challenge. If we measure the delay before packet discarding, the collected data will include the effects of MAC

Parameter	Value
Slot time (σ)	13 μs
SIFS	32 μs
DIFS	58 μs
MAC header (L_{MAC})	24 *bytes*
PHY header (L_{PHY})	4 *bytes*
UDP packet (E[P])	100 *bytes*, 300 *bytes*, 1053 *bytes*
Data Rate (R_d)	6 $Mbps$
Contention window (CW_0)	15
Propagation delay (δ)	1 μs
Transmission range (R)	300 m
Speed	30 m/s

Table 4.1: Parameter table

channel contention. In contrast, if we measure it after discarding, the collected delay reflects only the delay without MAC contention.

- Accurately tracking whether each node receives the packet is crucial for validating reliability in our simulations. To achieve this, we employed callback functions, which are triggered whenever a specified event occurs. This mechanism enables us to effectively monitor both the occurrence and the frequency of such events, providing essential insight into packet reception across the network. In our study, we employed four callback functions—"PhyRxBegin", "PhyRxEnd", "PhyRxDrop", and "MonitorSnifferTx"—to support the simulation and validation of reliability. Specifically, "PhyRxBegin" indicates that a packet signal is detectable at the physical layer with sufficient signal strength; "PhyRxEnd" confirms that the packet has been successfully received without collision; "PhyRxDrop" captures all dropped packets at the physical layer due to various errors or interference; and "MonitorSnifferTx" records the packet transmission behavior at the physical layer. By analyzing these callback functions and implementing corresponding handlers, we were able to systematically evaluate and verify the reliability of our network simulations.

- Since it is necessary to record the status of each individual vehicle, we configure the callback functions on a per-node basis, similar to the application layer setup. This ensures that each node independently monitors and logs its own transmission and reception events.

After overcoming these challenges, our simulation was successfully conducted. The table 4.1 lists the various parameters used in our simulation.

4.3 Results of Simulation Without MAC Contention

As illustrated in Figures 4.1 to 4.4, the model described by Equation 3.4 is employed. We evaluate different packet sizes ranging from 100 bytes to 400 bytes. It can be observed that, regardless of the packet size, the discrepancy between the simulation results and the theoretical values remains relatively constant. This is because the model in Equation 3.4 accounts only for the physical and MAC layer headers, whereas additional overhead

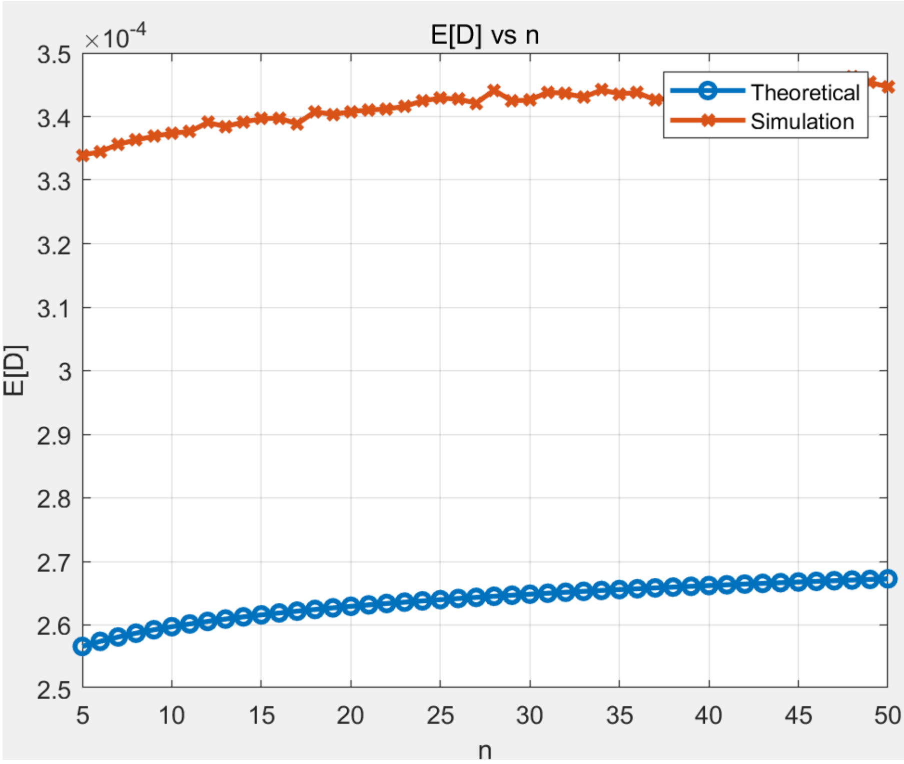

Figure 4.1: Packet Size is 100 bytes

from other network layers is not considered. Consequently, the observed gap is primarily attributed to the headers of upper-layer protocols.

The headers from the other layers are denoted as $E[S]$, and we calculate their size to be approximately 58.5 bytes. When $E[S]$ is added, the simulation results align with the theoretical values, as shown in Fig. 4.5. Figures 4.6 to 4.9 present the performance for each packet size.

4.4 Results of Simulation With MAC Contention

Given that the initial simulation did not account for MAC contention, we proceed to test the model under different parameters in the presence of MAC contention. The first two figures, Fig. 4.10 and Fig. 4.11, show the results of our work under different parameters. Although some parameters may cause relatively large differences, the discrepancies can be limited to within 0.2 ms. Here, we use three different packet sizes: 100 bytes, 300 bytes, and 1053 bytes. The 100-byte packet is used purely for testing purposes. The 300-byte packet represents the moderate size specified by the National Highway Traffic Safety Administration (NHTSA), and it is also used for testing purposes. The packet size of 1053 bytes is used based on the specifications provided by the National Highway Traffic Safety Administration (NHTSA), where the packet size range is defined between 200 and 500 bytes, with an average size of approximately 351 bytes. In this simulation, we model an emergency message consisting of three packets, which are sent consecutively without channel contention after the first packet is transmitted. Therefore, we use a packet size of 1053 bytes (approximately 351 bytes $\times$ 3) to test the model.

Figures 4.10 and 4.11 might be confusing, so we use the disassembled figures to better illustrate how our model works. In this test, we use the initial parameters, setting the

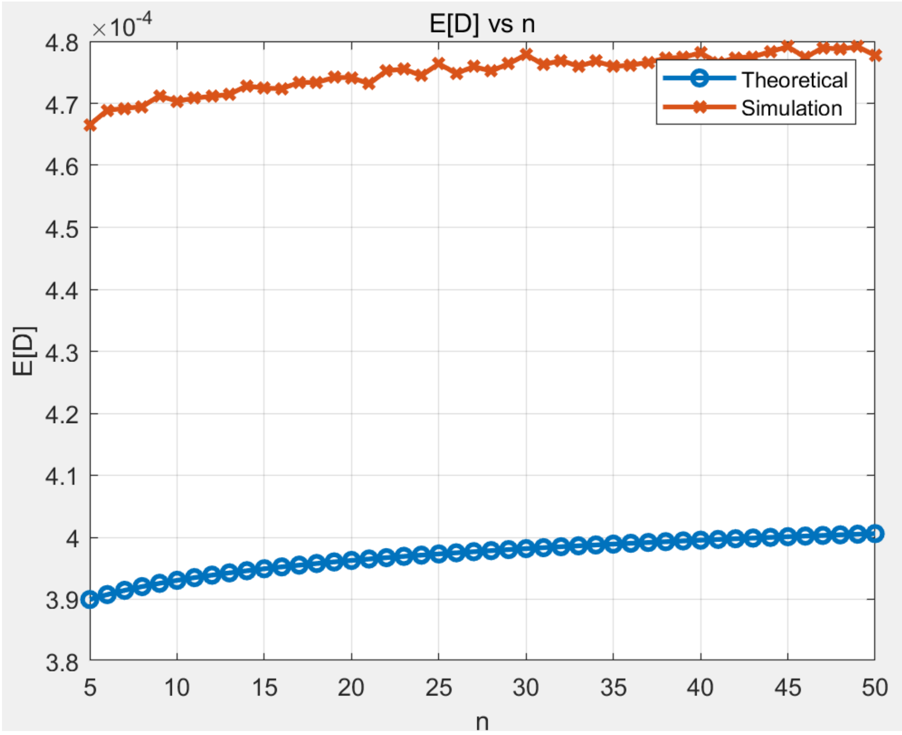

Figure 4.2: Packet Size is 200 bytes

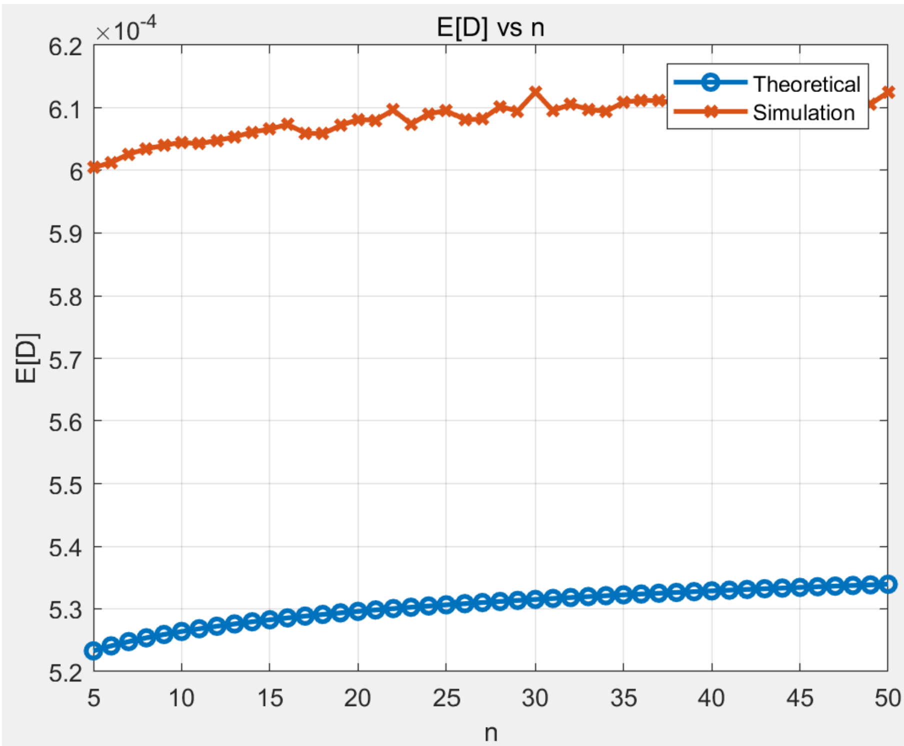

Figure 4.3: Packet Size is 300 bytes

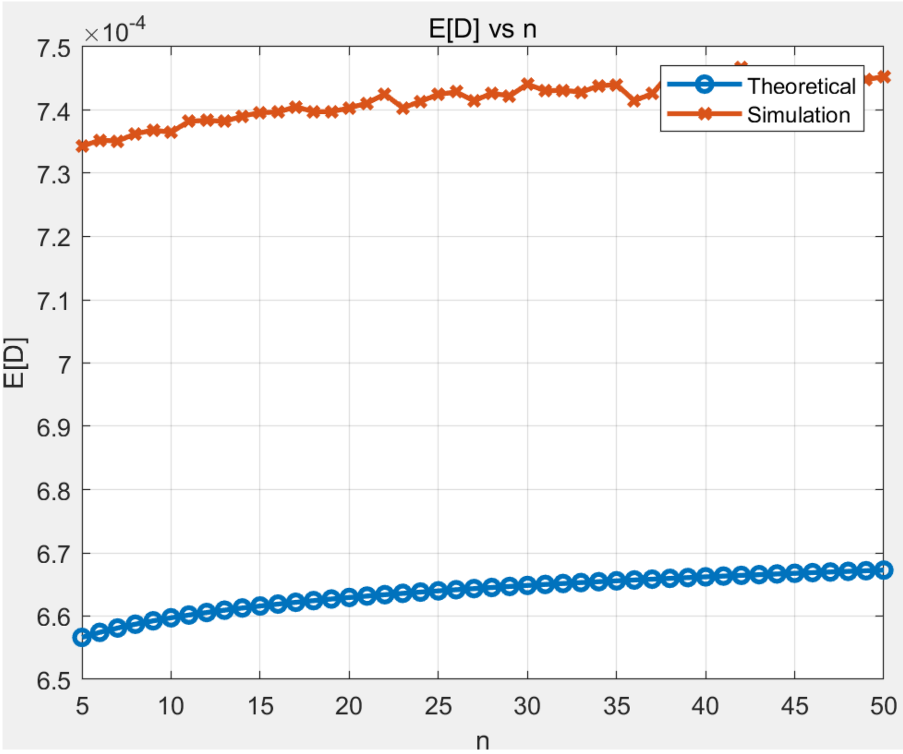

Figure 4.4: Packet Size is 400 bytes

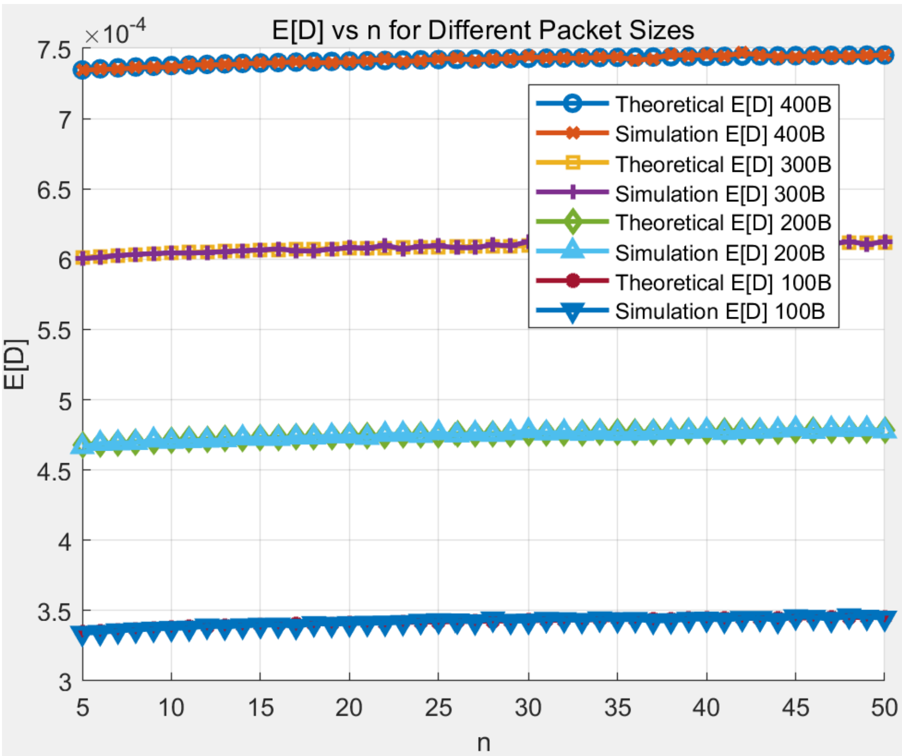

Figure 4.5: All packet size with E[S]

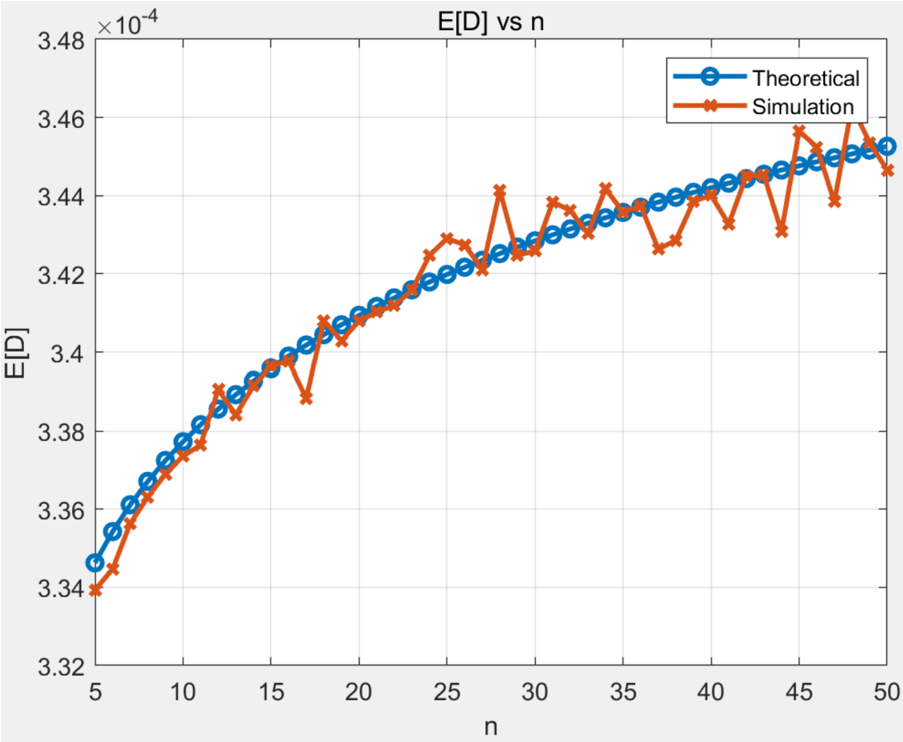

Figure 4.6: Packet Size is 100 bytes with E[S]

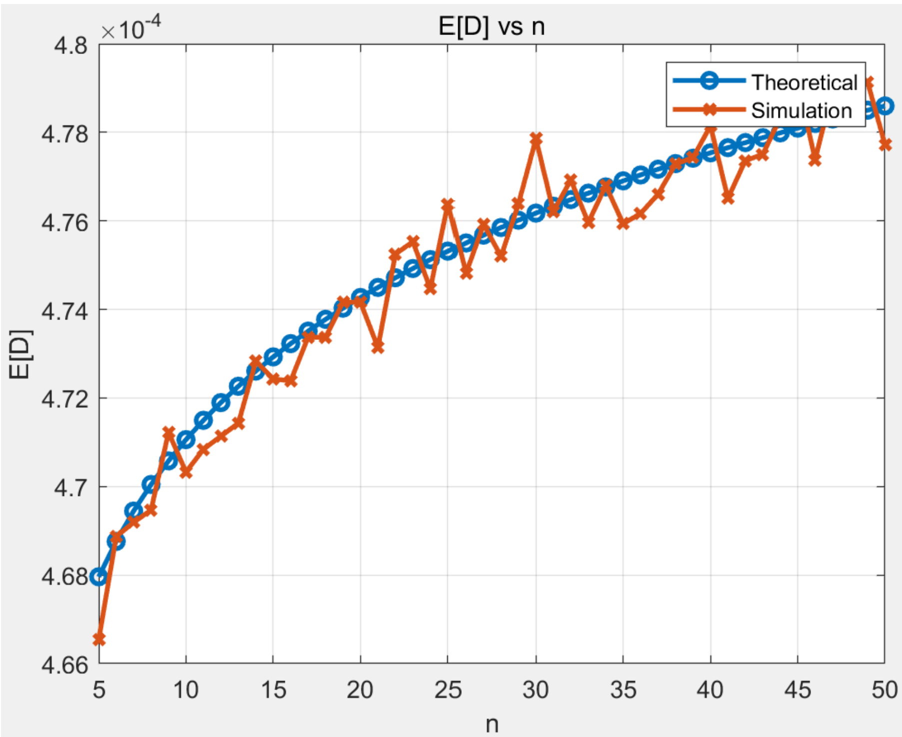

Figure 4.7: Packet Size is 200 bytes with E[S]

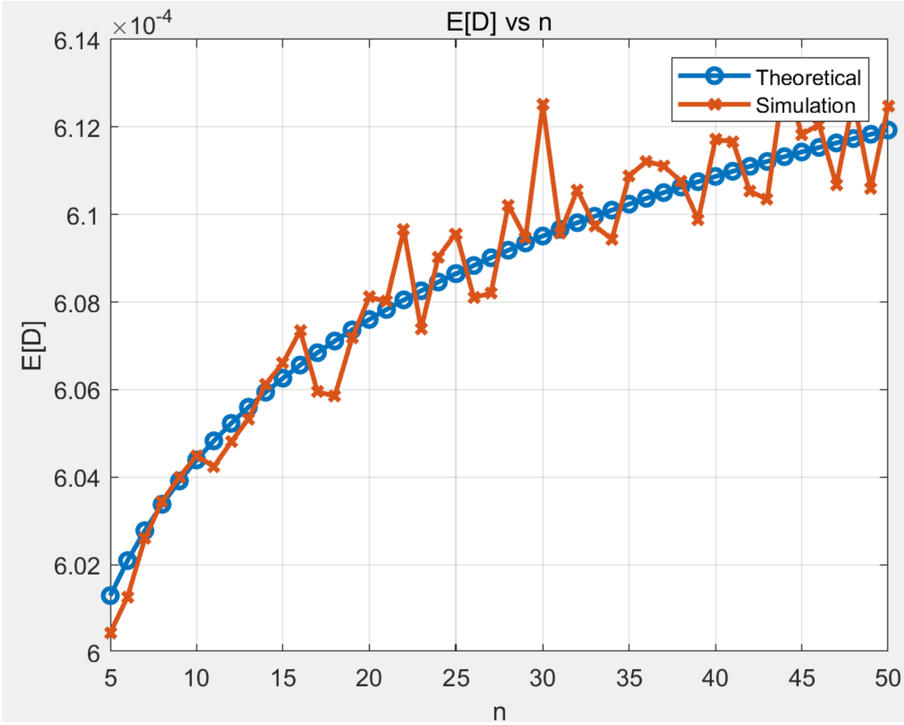

Figure 4.8: Packet Size is 300 bytes with E[S]

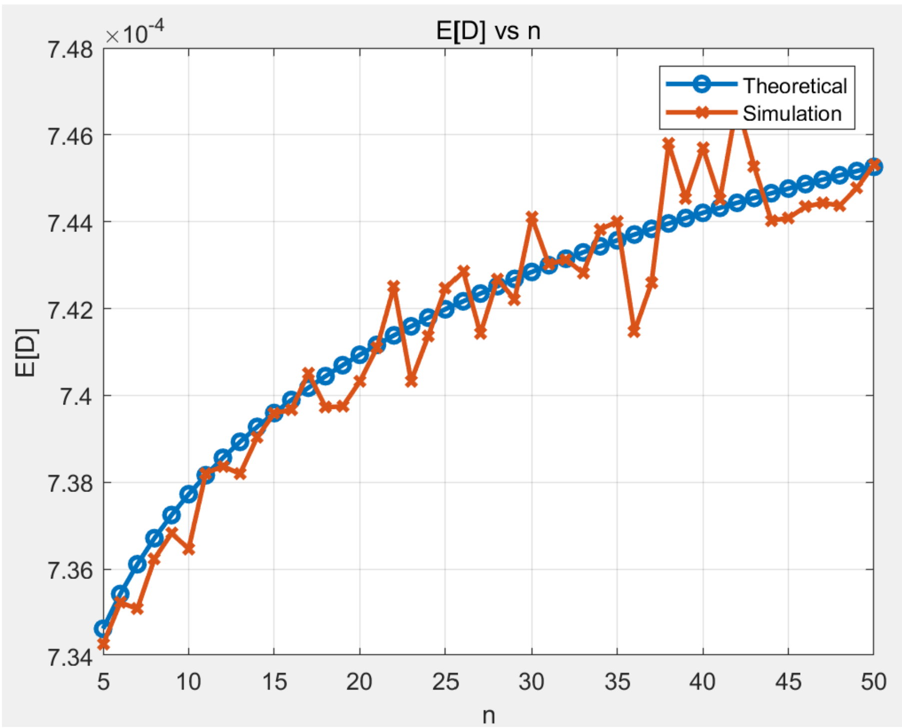

Figure 4.9: Packet Size is 400 bytes with E[S]

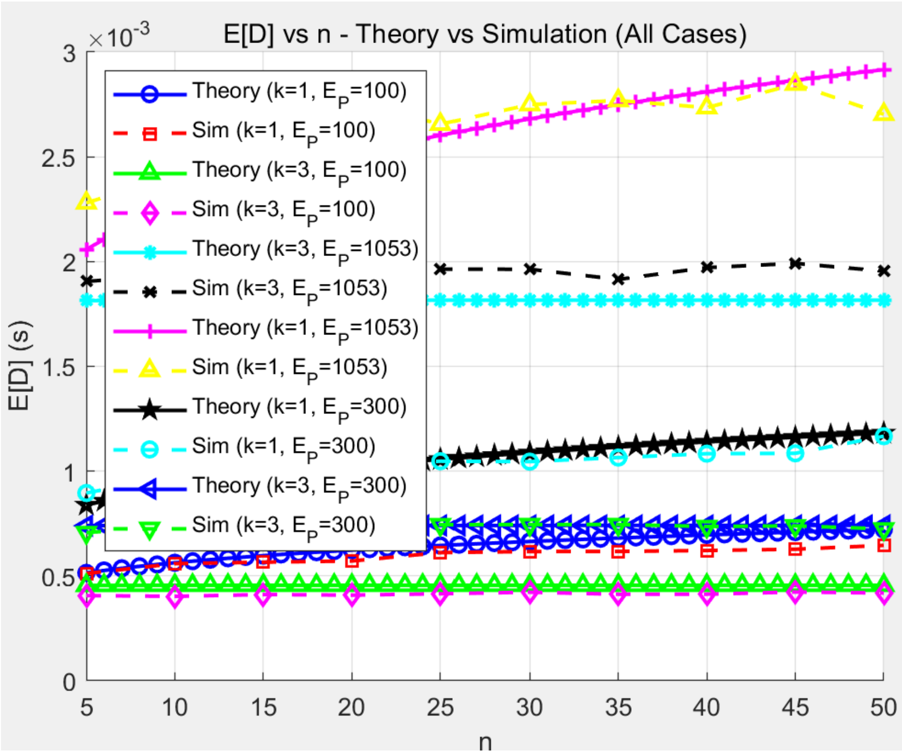

Figure 4.10: $\lambda = 0.9$

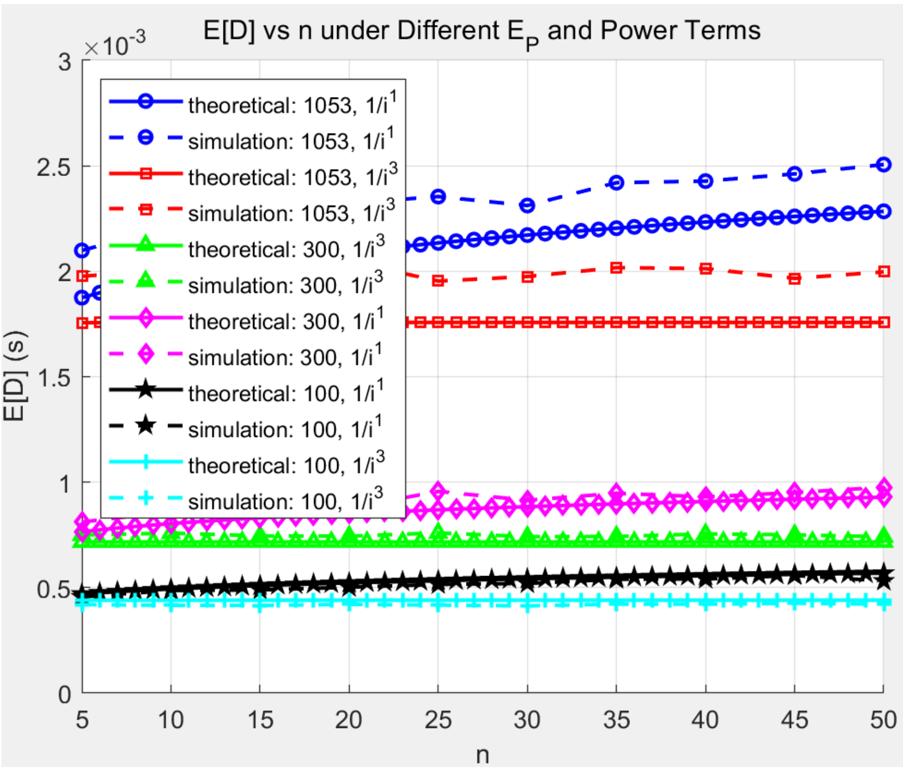

Figure 4.11: $\lambda = 0.6$

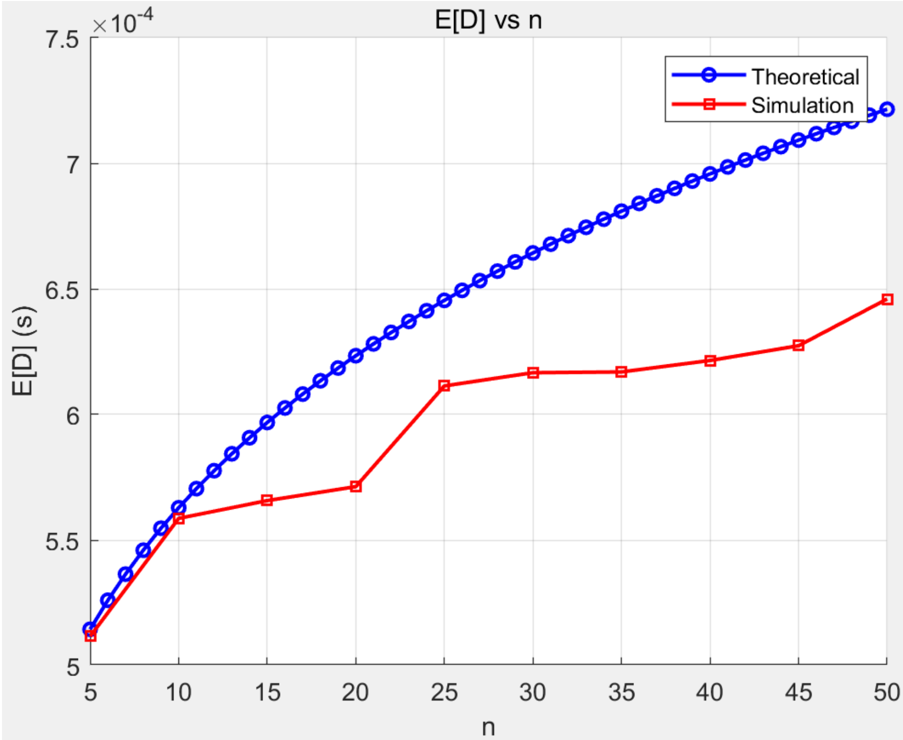

Figure 4.12: $\lambda = 0.9$, $k = 1.0$

packet size to 100 bytes. As Fig. 4.12 to 4.15.

As shown in Fig. 4.12, the average one-hop delay increases with the node density with $\lambda = 0.9$, $k = 1$.

As shown in Fig. 4.13, the rate of increase is lower than for $k = 1$ because the forwarding probability of all nodes decreases, except for the first node, resulting in a smaller network size compared to $k = 1$. The Fig. 4.14 and 4.15 has the similar illustration but their have lower $E[D]$ because lower forwarding probability on each node.

4.5 Compare The Model With FPBCSN

Here, we compare our work with the model proposed in [13]. igures 4.16 to 4.19 demonstrate that the model in [13] significantly underestimates the average one-hop delay. In [13], different broadcast probabilities were assigned to individual nodes in order to reduce the network size, leading to a very small overall channel busy probability p_b. As a result, the model is unable to provide a sufficiently large delay estimation.

Moreover, although each forwarder undergoes a fixed freeze period T regardless of the value of p_b, the model in [13] does not adequately reflect the impact of the freeze period when p_b becomes too small. Therefore, the theoretical values predicted by the model are considerably lower than the actual simulation results, leading to a significant underestimation of the average one-hop delay.

4.6 Results of Simulation With Reliability

Since simulating every possible distance would be overly complex, we perform simulations at 30-meter intervals to evaluate whether our reception rate model performs as expected.

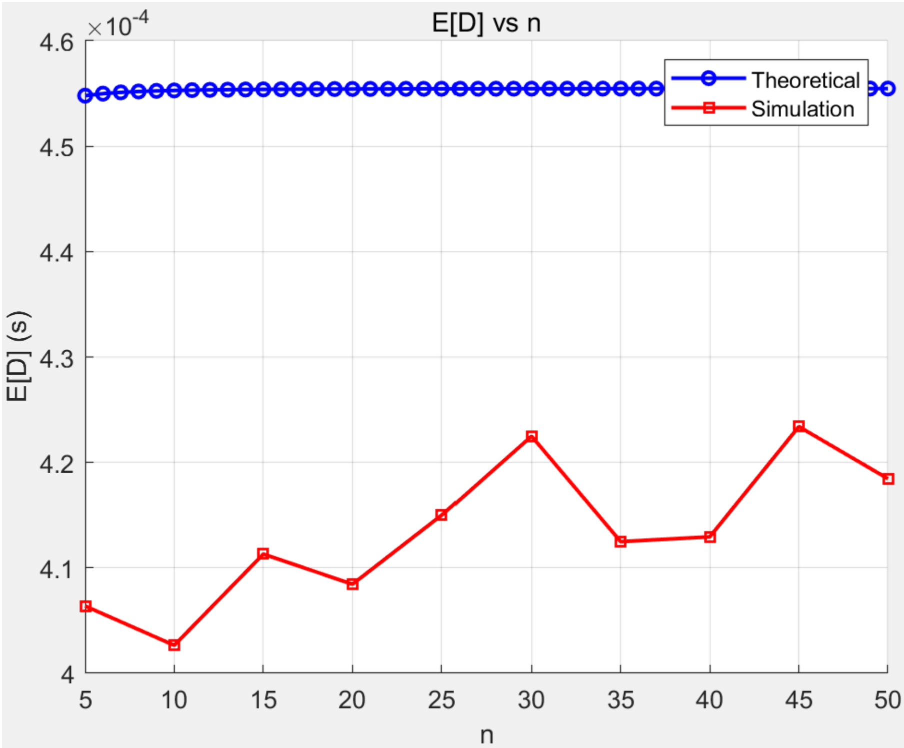

Figure 4.13: $\lambda = 0.9$, $k = 3.0$

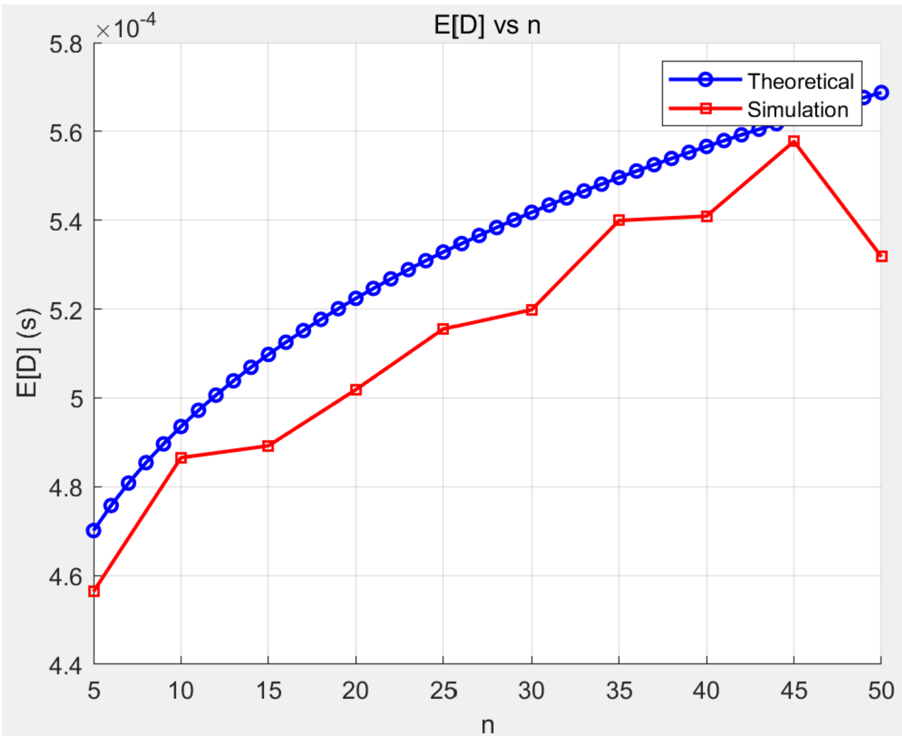

Figure 4.14: $\lambda = 0.6$, $k = 1.0$

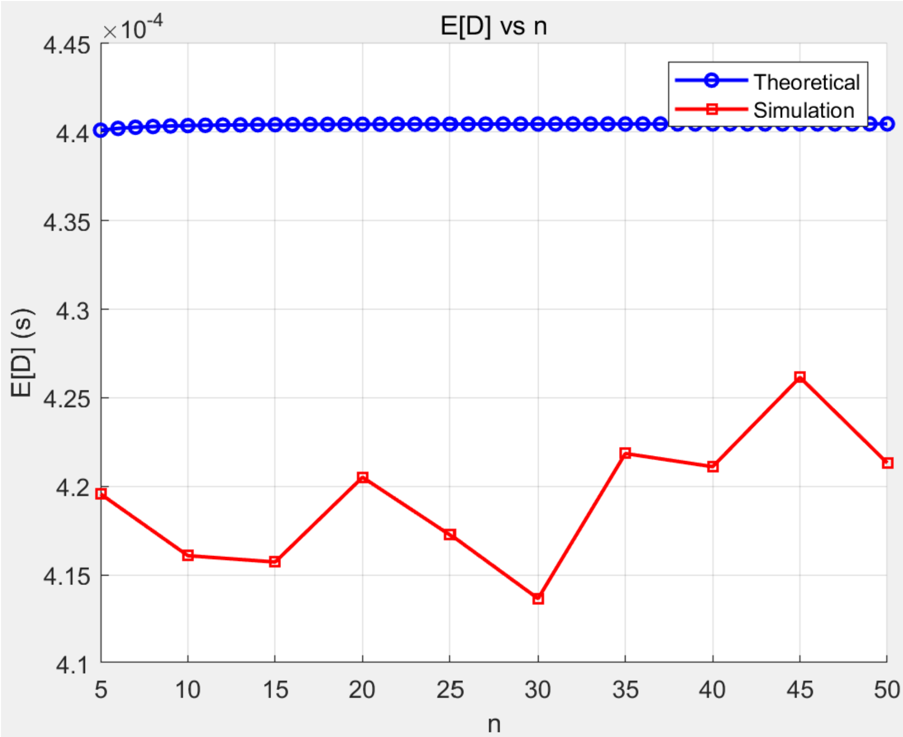

Figure 4.15: $\lambda = 0.6$, $k = 3.0$

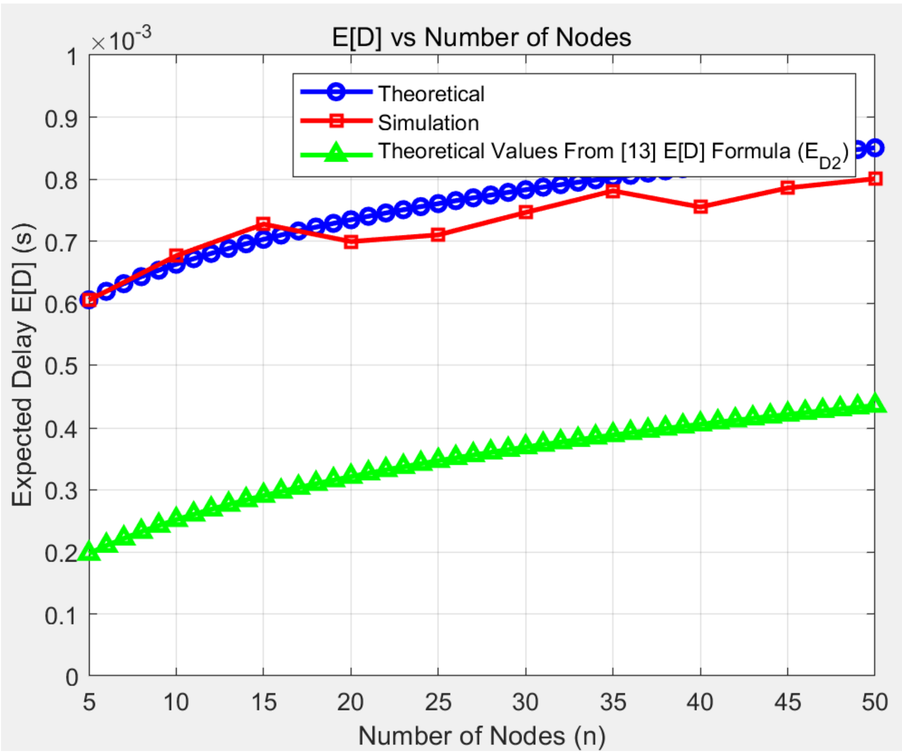

Figure 4.16: $\lambda = 0.9$, $k = 1$

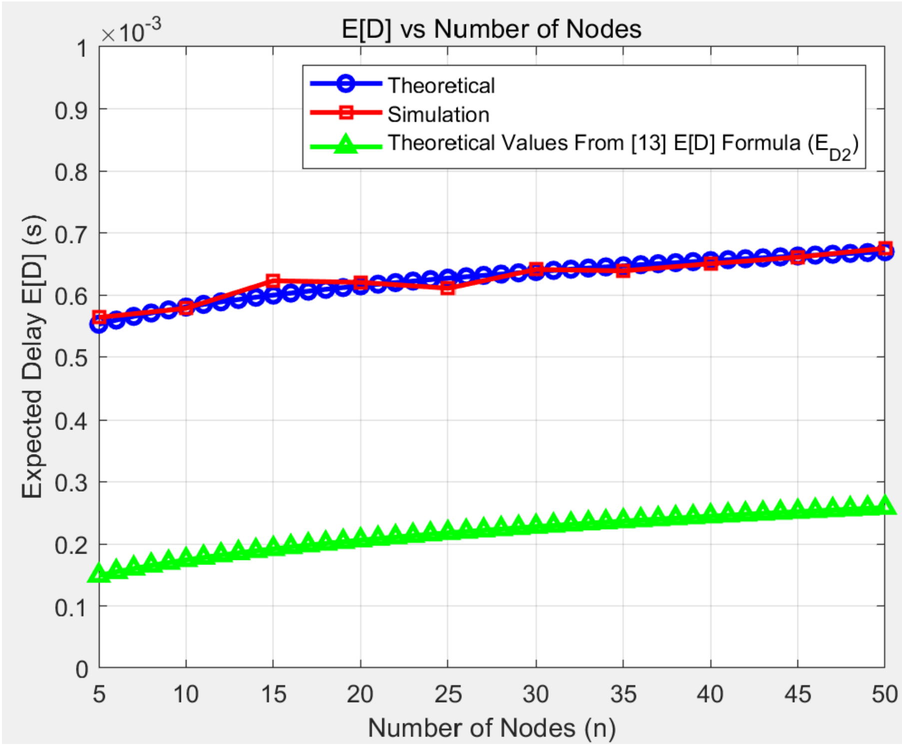

Figure 4.17: $\lambda = 0.6$, $k = 1$

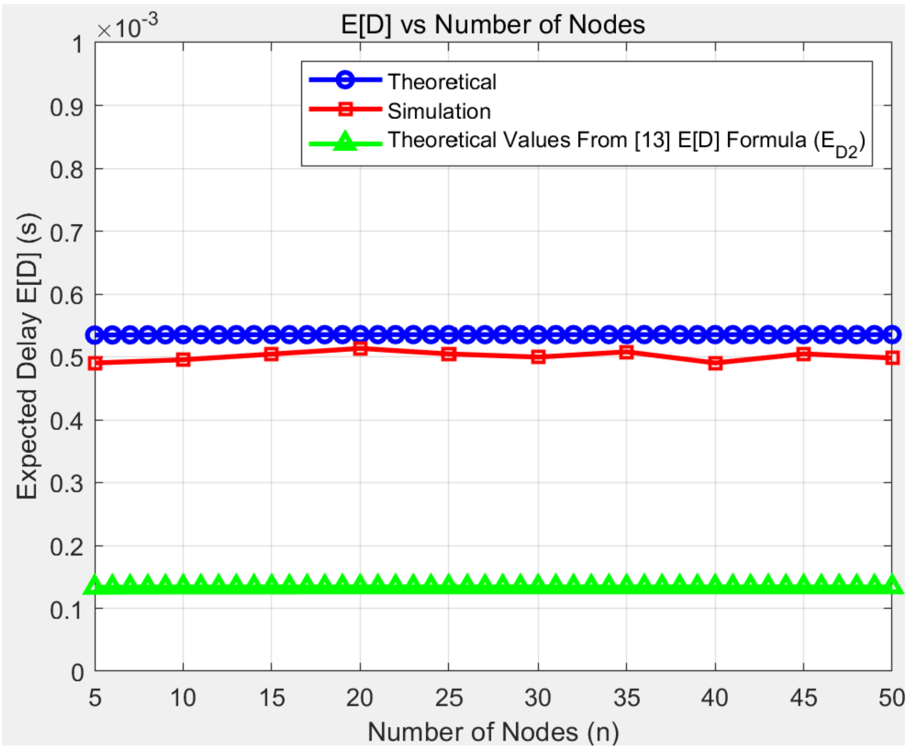

Figure 4.18: $\lambda = 0.9$, $k = 3$

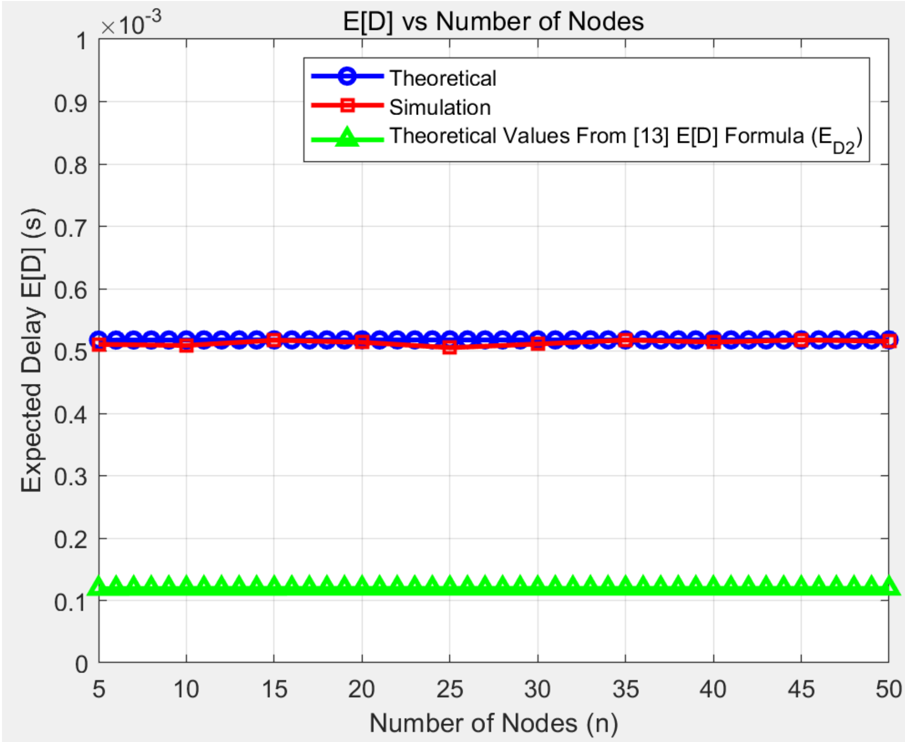

Figure 4.19: $\lambda = 0.6$, $k = 3$

Parameter	Value
Distance (d)	0-300 m
Reference Distance (d_0)	1 m
Path Loss Exponent (n)	3
Reference Loss ($PL(d_0)$)	47.8 dBm

Table 4.2: Logdistance Path Loss Parameter Table

Table 4.2, 4.3 and 4.4 include our simulation parameters.

In our simulation, we employ a simple two-node configuration, where one node acts as the sender and the other as the receiver. The receiver is placed at different distances to assess the impact of distance on signal reception. Although the reception threshold was set to -89 dBm, practical tests showed that when only the Log-Distance Path Loss Model was used, a received power of at least -82 dBm was required to ensure successful packet reception, likely due to additional factors such as bit error rate (BER) and other sources of interference.

4.7 Results of Simulation With Coverage

Figures 4.20 and 4.21 demonstrate that our work performs consistently well, exhibiting nearly identical trends in terms of incremental growth and magnitude. In this work, we consider the case where $k = 1$, with λ set to 0.9 and 0.6, respectively. The number of retransmissions is set to 3, and the packet size is 156 bytes. All other parameters are configured according to Table 4.1.

In Figures 4.20 and 4.21, it can be observed that the theoretical values are consistently lower than the simulation results. This discrepancy also persists when the value of

Parameter	Value
m_0	1.5
m_1	0.75
m_2	0.5
Distance1 (m_0)	within 100 m
Distance2 (m_1)	over 100 m within 200 m

Table 4.3: Nakagami Parameter Table

Parameter	Value
Transmit Power	22.5 dBm
RxGain	17.65 dBm
TxGain	0 dBm
RxSensitivity	-89 dBm

Table 4.4: Transmit and Receive Parameter table

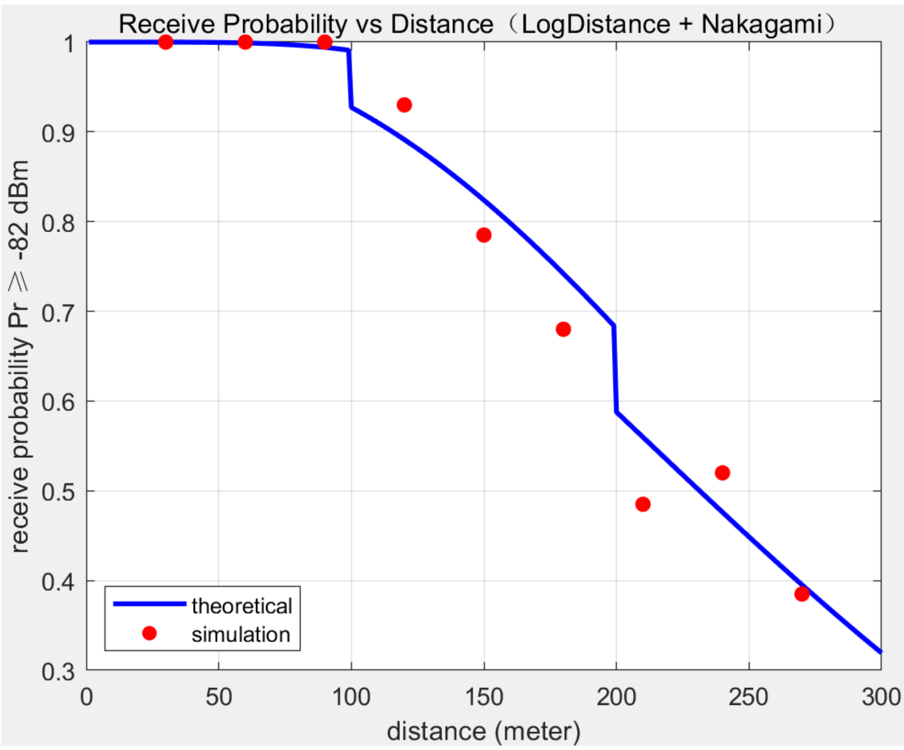

Figure 4.20: Receive Probability Theoretical and Simulation

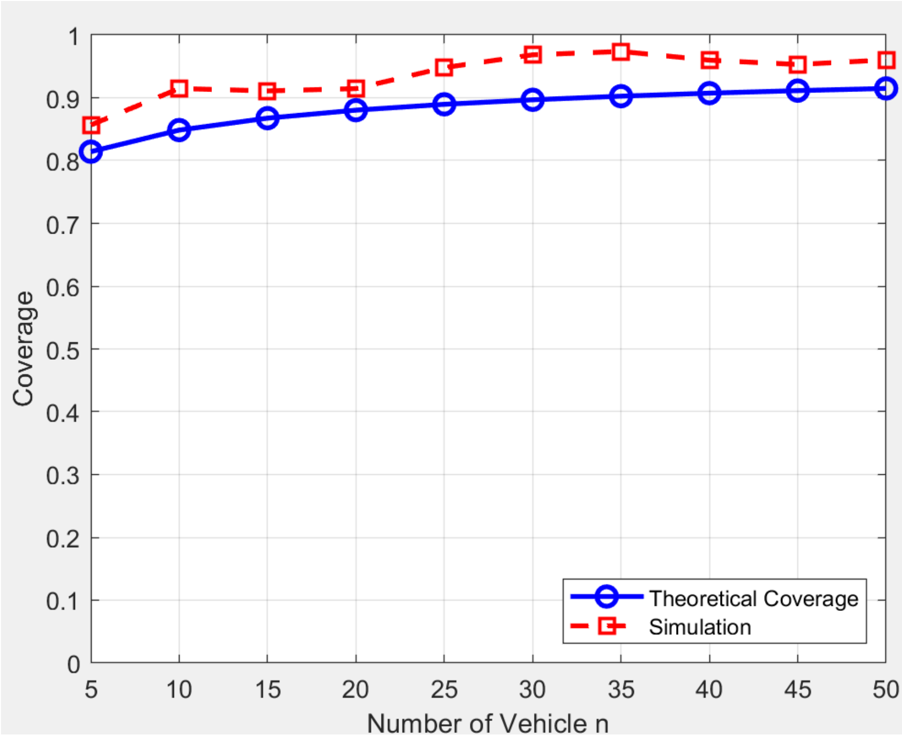

Figure 4.21: Coverage for $\lambda = 0.9$, $k = 1$

k increases. This deviation is likely due to the fine-grained nature of our reception probability calculation, which may lead to a conservative estimate and consequently result in lower theoretical values compared to simulation outcomes.

4.8 Summary

To improve the generality of our findings, each node in the simulation is configured to transmit the packet three times. To model the average one-hop delay more accurately, it is necessary to allow each vehicle to transmit multiple packets, here we let each forwarding nodes and source send packet three times. If each vehicle sends only one packet, MAC layer contention would have minimal influence on the results, as each node would only receive the earliest transmitted packet. Therefore, in our simulation, each node records the delay of every received packet, while redundant packets (i.e., those with the same packet ID) are discarded at the application layer. Although the first received packet may not experience significant MAC layer contention, the subsequent two transmissions are more likely to trigger contention due to concurrent access attempts. As a result, the delays recorded from the later packets help offset the minimal contention observed in the initial packet, thereby yielding a more representative average one-hop delay. Therefore, we record the one-hop delay for each individual packet to ensure that the computed average reflects typical network conditions.

In order to assess the reliability of message transmission, we incorporate a lossy channel fading model that reflects the possibility of packet loss due to real-world wireless propagation impairments. With the inclusion of a stochastic fading model (Nakagami-m), computing the average reception probability across different road segments characterized by distinct fading parameters becomes a primary objective in our investigation

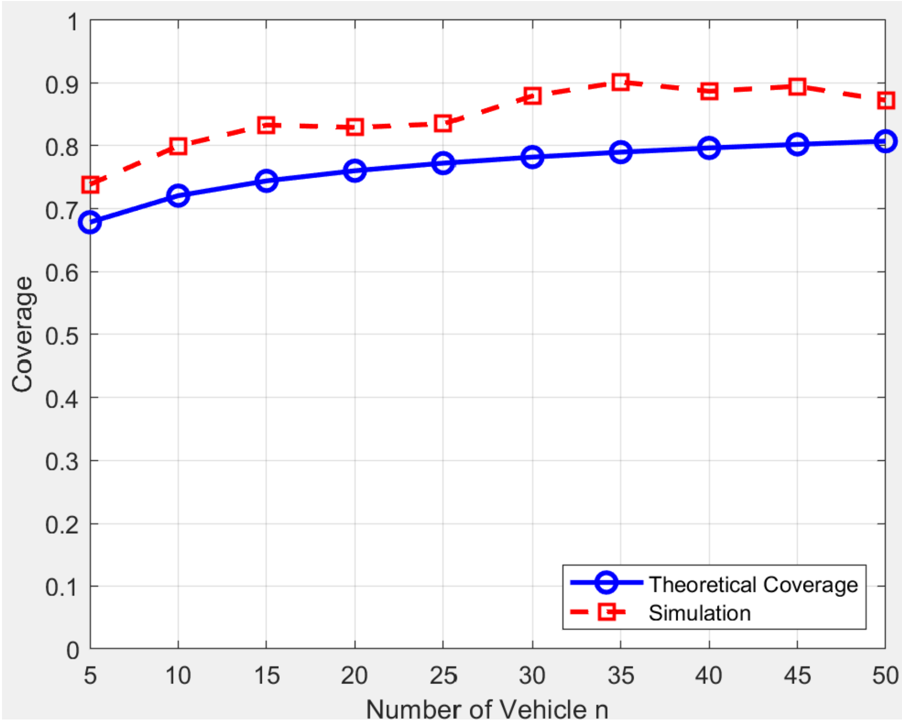

Figure 4.22: Coverage for $\lambda = 0.6$, $k = 1$

of reliability. In this context, a finer granularity in interval partitioning during modeling—i.e., computing expectations over smaller sub-intervals rather than a single broad range—enhances the precision and fidelity of the model.

Coverage is derived based on the reliability analysis, as our primary objective is to ensure that following vehicles receive critical messages as promptly and reliably as possible. Therefore, we model the coverage within a limited time and distance to evaluate how effectively messages are disseminated throughout the network when using the FPBCSN protocol. Although our model tends to slightly underestimate the actual performance, this conservative estimation introduces a margin of engineering redundancy. As a result, the network can achieve a higher theoretical coverage in practical deployments, which helps accommodate unforeseen interference and other adverse conditions.

Chapter 5

Conclusion

In our work, we propose two models: one for average one-hop delay under varying node densities, and another for reliability when node density is fixed and the protocol coefficient k is relatively large, focusing on how reliability changes with different values of λ, and find for different vehicle density, the model working normally bar.

Future work should aim to optimize computational efficiency while maintaining acceptable average one-hop delay and high reliability. Moreover, a deeper investigation into how reliability evolves with broader variations in node density is necessary, along with the development of more adaptable models. As our current model is based on a limited density range, its applicability under higher-density scenarios remains uncertain, which may significantly affect the timely and reliable dissemination of emergency messages in vehicular networks.

Bibliography

[1] L. Briesemeister and G. Hommel, *Role-based multicast in highly mobile but sparsely connected ad hoc networks*, Proc. ACM Symp. Mobile Ad Hoc Netw. Comput., Aug. 2000.

[2] G. Korkmaz, E. Ekici, F. Ozguner, and U. Ozguner, *Urban multi-hop broadcast protocol for inter-vehicle communication systems*, Proc. 1st ACM Int. Workshop Veh. Ad Hoc Netw, 2004.

[3] M.-C. Chuang and M. C. Chen, *DEEP: Density-aware emergency message extension protocol for VANETs*, IEEE Trans. Wireless Commun, vol. 12, no. 10, pp. 4983–4993, Oct. 2013.

[4] H. Yoo and D. Kim, *ROFF: Robust and fast forwarding in vehicular ad-hoc networks*, IEEE Trans. Mobile Comput., vol. 14, no. 7, pp. 1490–1502, Jul. 2015.

[5] T. B. Achour and S. Tabbane, *Network coding approach for vehicle-tovehicle communication: Principles protocols and benefits*, in Proc. 22nd Int. Conf. Softw. Telecommun. Comput. Netw, 2014, pp. 154–159.

[6] L. Li, R. Ramjee, M. Buddhikot, and S. Miller, *Network coding-based broadcast in mobile ad-hoc networks*, in Proc. IEEE INFOCOM, 2007, pp. 1739–1747.

[7] C. Fragouli, J. Widmer, and J.-Y. L. Boudec, *Efficient broadcasting using network coding*, IEEE/ACM Trans. Netw., vol. 16, no. 2, pp. 450–463, Apr. 2008.

[8] N. Wisitpongphan, O. K. Tonguz, J. S. Parikh, P. Mudalige, F. Bai, and V. Sadekar, *Broadcast storm mitigation techniques in vehicular ad hoc networks*, IEEE Wireless Commun. Mag., vol. 14, no. 6, pp. 84–94, Dec. 2007.

[9] L. Zhou, G. Cui, H. Liu, Z. Wu, and D. Luo, *Nppb: A broadcast scheme in dense vanets*, Inf. Technol. J., vol. 9, no. 2, pp. 247–256, 2010.

[10] S. Panichpapiboon and G. Ferrari, *Irresponsible forwarding*, in Proc. 8th IEEE Int. Conf. ITS Telecommun., 2008, pp. 311–316.

[11] S. Panichpapiboon, *Irresponsible forwarding under general inter-vehicle spacing distributions*, in Proc. 8th Int. Conf. Electric. Eng./Electron., Comput., Telecommun. Inf. Technol., 2011, pp. 357–360.

[12] A. Mostafa, A. M. Vegni, and D. P. Agrawal, *A probabilistic routing by using multihop retransmission forecast with packet collision-aware constraints in vehicular networks*, Ad Hoc Netw., vol. 14, no. 12, pp. 118–129, Mar. 2014.

[13] X. Ma and X. Chen, *Performance Analysis of IEEE 802.11 Broadcast Scheme in Ad Hoc Wireless LANs*, IEEE Trans. Veh. Technol., vol. 57, no. 6, pp. 3757–3768, Nov. 2008.

[14] G. Bianchi, *Performance analysis of the IEEE 802.11 distributed coordination function*, IEEE J. Sel. Areas Commun., vol. 18, no. 3, pp. 535–547, Mar. 2000.

[15] D. Malone, K. Duffy, and D. Leith, *"Modeling the 802.11 distributed coordination function in nonsaturated heterogeneous conditions*, IEEE J. " IEEE/ACM Trans. Netw., vol. 15, no. 1, pp. 159–172, Feb. 2007.

[16] X. Zeng, M. Yu, and D. Wan, *A new probabilistic multi-hop broadcast protocol for vehicular network*, IEEE Trans. Veh. Technol., vol. 67, no. 12, pp. 12165–12171, Dec. 2018.

[17] Francisco J. Ros, Pedro M. Ruiz, and Ivan Stojmenovic, *Reliable and Efficient Broadcasting in Vehicular Ad Hoc Networks*, VTC Spring 2009-IEEE 69th Vehicular Technology Conference, 2009.